Chemica Scripta. Vol. 21, 43–53, 1983.

The Metal Centers of Cytochrome c Oxidase: Structures and Interactions

David F. Blair, Craig T. Martin, Jeff Gelles, Hsin Wang, Gary W. Brudvig, Tom H. Stevens and Sunney I. Chan

A. A. Noyes Laboratory of Chemical Physics, 127-72, California Institute of Technology, Pasadena, California 91125, U.S.A.

Received September 10, 1982

Paper presented at the Nobel Symposium "Inorganic Biochemistry", Karlskoga, Sweden, September 5–10, 1982

Abstract

Studies directed toward the elucidation of the structures of the metal centers in cytochrome *c* oxidase are reviewed. Progress towards an understanding of the interactions between these centers and their spatial distributions within the protein will also be presented. Our studies are based primarily on optical and low-temperature electron paramagnetic resonance (EPR) spectroscopy. We have employed nitric oxide (NO), as well as other exogenous ligands, to probe the O_2 reduction site of the enzyme. In addition, we have isolated auxotrophs of *Saccharomyces cerevisiae* in order to metabolically incorporate isotopically substituted amino acids into the yeast protein. Low-temperature EPR and electron nuclear double resonance (ENDOR) spectroscopic studies of these isotopically substituted derivatives have provided unambiguous information on the structure of two of the four metal centers. The degree to which metal centers within the protein interact with one another has been assessed by examining the extent to which redox changes of one metal center modulate changes in the EPR and optical characteristics of the other centers. Conceptions about the overall spatial distribution of the metal centers within the protein emerge from these data. The implications of our results with respect to the mechanisms of dioxygen reduction and energy conservation in cytochrome *c* oxidase will be discussed.

Introduction

Cytochrome *c* oxidase is the terminal enzyme in the respiratory chain of eukaryotic organisms. It catalyzes two energy-linked chemical reactions: the generation of an electrochemical hydrogen ion gradient across the mitochondrial membrane in which the enzyme resides, and the transfer of four electrons from ferrocytochrome *c* to dioxygen (eq. (1); $\Delta G^{0'} = -55$ kcal mol^{-1}) [1]. The free energy released by the latter reaction under physiological

$$O_2 + 4 \text{ ferrocytochrome } c + 4H^+ \rightarrow 2H_2O + 4 \text{ ferricytochrome } c \quad (1)$$

conditions provides the driving force for the former energetically unfavorable one. In living cells, these reactions occur rapidly [2], in a highly energy-efficient manner, and without substantial production of hydroxyl radicals or other toxic intermediates of oxygen reduction.

One of the major goals of researchers studying cytochrome oxidase has been the elucidation of the chemical mechanisms of the redox processes catalyzed by the enzyme. These include the details of the entry of electrons into and the flow of electrons through the enzyme as well as the steps by which O_2 is reduced to H_2O at the oxygen binding site of the enzyme. All indications are that the oxidase receives its reducing equivalents from cytochrome *c* on the cytosol side, while the four protons which are consumed per turnover originate in the matrix. In this manner, four negative charges are transferred across the inner membrane and a transmembrane electrochemical potential gradient is established. Evidence is mounting that the enzyme is also a proton pump with protons pumped across the inner membrane from the matrix to the cytosol during the electron transport and/or O_2 reduction processes [3]. The number of protons (four to eight) pumped per turnover, however, remains unclear.

The structure of the protein has naturally received considerable attention. Impressive progress has been made toward deciphering the primary sequence and the subunit structure of the enzyme [4]. A glimpse of the three-dimensional folding and assembly of the protein (Fig. 1) has also emerged from electron microscopy imaging studies [5]. The structures of the four metal centers that are intimately associated with the electron transfer, O_2 reduction, and possibly proton pumping, are beginning to be understood.

In this report, we will review our efforts toward elucidating the structures of and the interactions between the four metal centers in cytochrome *c* oxidase. Our studies are based largely on optical absorption and low-temperature electron paramagnetic resonance (EPR) spectroscopy. We have used nitric oxide (NO) and other exogenous ligands to probe the structure of the O_2 reduction site. In addition, we have prepared isotopically substituted enzyme derivatives from the yeast *Saccharomyces cerevisiae* and studied them by electron nuclear double resonance (ENDOR) spectroscopy. These approaches have provided unambiguous information on the ligands of two of the four metal centers as well as information regarding the spatial relationships of the metal centers. The structural results reviewed here have furnished valuable insights into the mechanism of dioxygen reduction by this enzyme. We feel that an important

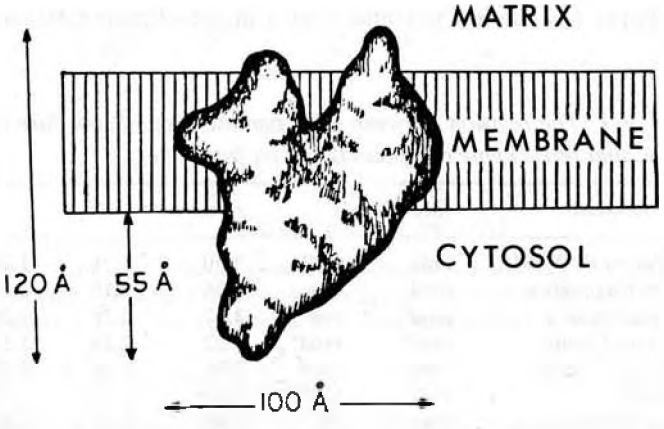

Fig. 1. Three-dimensional folding and assembly of oxidized cytochrome *c* oxidase as revealed by electron microscopy imaging.

beginning has been made and are optimistic that a detailed picture of the structure and function of cytochrome *c* oxidase is on the horizon.

Structure of the cytochrome *c* oxidase metal centers

Cytochrome *c* oxidase contains four inequivalent metal centers, each of which accepts a single electron in the conversion of the enzyme from the fully oxidized to the fully reduced state [2]. Two of the centers are heme A, a unique iron porphyrin with a formyl group and a hydrophobic isoprenoid side chain. The other two metal centers are unusual copper ions which are structurally and spectroscopically different from one another and distinct from any of the types 1, 2, or 3 coppers found in laccases and other cuproproteins. The metal ions which comprise the O_2 binding site (Fe_{a_3} and Cu_B) both have the capacity to bind exogenous ligands such as HCN and NO. The other two metal ions (Fe_a and Cu_A) are shielded from interaction with added ligands and serve to mediate the transfer of electrons between cytochrome *c* and the oxygen reduction site. We now describe in turn results relating to the structure of each of these metal centers.

Cytochrome a

There seems to be general agreement that cytochrome *a* (Fe_a) accepts electrons from ferrocytochrome *c* and transfers them to the Cu_A center. The cytochrome *c* binding site(s) is located on the cytosol side of the inner mitochondrial membrane [6]. The reduction potential of Fe_a is similar to that of cytochrome *c*, which is expected if Fe_a is the point of entry of electrons into the protein and degradation of the redox free energy is to be minimized in this electron transfer step [7].

All indications are that Fe_a is six-coordinate and low-spin, with nitrogens from two neutral imidazoles as axial ligands. Such a structure would be consistent with the proposed electron transfer function of Fe_a. The magnetic circular dichroism (MCD) and EPR spectra of Fe_a demonstrate clearly that Fe_a is low-spin [8, 9]. There have been two lines of evidence supporting two histidine imidazoles as axial ligands. Babcock *et al.* [10] have compared the optical and resonance Raman spectra of Fe_a with those of related low-spin heme A models. Similarly, Peisach [11] has compared the *g*-values of Fe_a with those of low-spin heme A models with known axial ligands. The Peisach compilation of *g*-values is reproduced in Table I. The *g*-values (3.0, 2.21, 1.45) of Fe_a (Fig. 2) are reproduced only by the *bis* neutral–imidazole complex of heme A.

Copper A

Copper A is the low potential copper in cytochrome *c* oxidase,

Table I. *The relation between EPR parameters and structure of low spin ferric heme compounds (taken from [11])*

Compound	Axial ligands		*g* values		
Glycera Hb $MeNH_2$	imid	RNH_2	3.30	1.98	1.20
Leg Hb pyridine	imid	pyr	3.26	2.10	0.82
Cytochrome *c*	imid°	met	3.07	2.26	1.25
Bis imid heme	imid°	imid°	3.02	2.24	1.51
Bis $imid^-$ heme	$imid^-$	$imid^-$	2.80	2.26	1.72
MbOH	$imid^-$	OH^-	2.55	2.17	1.85
Cyt. P-450_{cam}	imid°	RS^-	2.45	2.26	1.92
Cyt. *c* oxidase	imid°	imid°	3.0	2.2	1.5

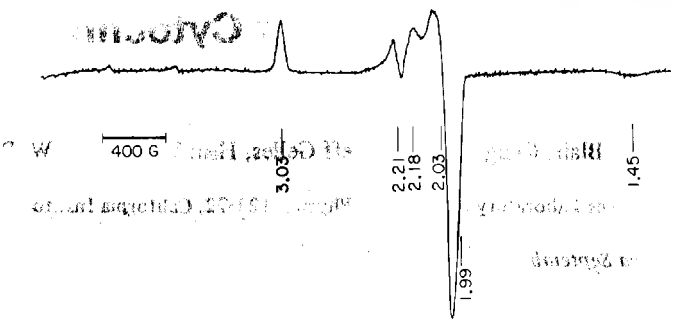

Fig. 2. X-band EPR spectrum of oxidized beef heart cytochrome *c* oxidase at 10 K.

and it has been suggested that the function of this metal center is to transfer electrons from Fe_a to the O_2 reduction site. Its reduction potential [7] is similar to that of Fe_a. Since the first reduction potential drop occurs between Cu_A and the O_2 reduction site, Chan *et al.* have proposed that this redox energy may be conserved and that Cu_A might serve as the proton pump of the enzyme [12].

Cu_A displays an unusually isotropic EPR spectrum with no hyperfine splitting resolved when the spectrum is recorded at 9 GHz (Fig. 2). Computer simulations of this spectrum [13, 14] generate a good fit using *g*-values of 2.18, 2.03, and 1.99. The latter *g*-value has been of particular interest as it is below that of the free electron (2.0023), a situation which is not possible for simple Cu(II) centers [15]. X-ray absorption edge data indicate that the oxidized Cu_A center is in a highly covalent environment and that the copper might even be reduced to Cu(I) [16]. Substantial delocalization of spin onto an associated ligand in the oxidized enzyme could explain these results [17].

ENDOR studies have shown hyperfine interactions between the unpaired electron and various nuclei. Copper ENDOR has been reported [18], indicating an unusually small and isotropic copper hyperfine interaction. In addition, ENDOR studies have demonstrated a ^{14}N hyperfine coupling of 17 MHz and two strong ^1H couplings of 12 and 19 MHz, respectively [19]. It has been proposed that these strongly coupled protons are the β-CH_2 protons of an associated cysteine ligand [19], in which case substantial spin density must reside on the cysteinyl sulfur (*vide infra*). If this is true, another polarizable ligand, such as a second cysteine, would be required [20] to render this transfer of electron density from ligand to metal energetically favorable.

These considerations led us to propose some years ago [17] that the Cu_A center in cytochrome *c* oxidase consisted of a Cu(I) ion ligated by two cysteinyl sulfurs, one a cysteinate and the other a sulfur radical. We have now undertaken experiments [21] to test this model by incorporating cysteine substituted with ^2H at the β-methylene carbon ((^2H)Cys) into yeast cytochrome *c* oxidase using a cysteine auxotroph of the yeast *Saccharomyces cerevisiae*. A histidine auxotroph was also isolated and used to incorporate histidine substituted with ^{15}N at both imidazole ring positions ((^{15}N)His) into the yeast enzyme. Our strategy in preparing these enzyme derivatives is to exploit the differences in nuclear spin and nuclear magnetic moment of the isotopes to identify magnetic interactions between the unpaired electron spin and the nucleus in question. Thus, perturbation of the EPR spectrum of the metal center by the isotopic substitution or, in the case where the hyperfine interaction is too

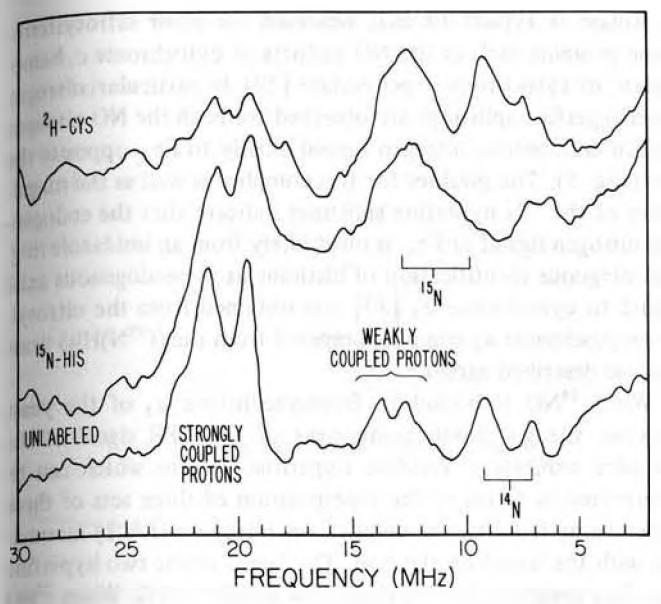

Fig. 3. ENDOR spectra of native, (^{15}N)His and (^{2}H)Cys yeast cytochrome *c* oxidase observed at $g = 2.04$, microwave frequency 9.12 GHz and temperature 2.1 K.

small to be discernible in the EPR, modification of the ENDOR spectrum may be used to obtain unambiguous information about the involvement of the particular amino acid at the site.

We have compared the EPR spectra of native, (^{2}H)Cys, and (^{15}N)His yeast cytochrome *c* oxidase. Differences were noted between the EPR spectra of Cu_A in the native and the isotopically substituted yeast proteins, implicating at least one histidine and one cysteine as ligands to Cu_A. Recent ENDOR studies carried out in collaboration with Dr C. P. Scholes of SUNY at Albany [21] confirmed these assignments. The Cu_A ENDOR spectra of (^{2}H)Cys and (^{15}N)His yeast oxidase are compared with that of the native yeast enzyme in Fig. 3. We note that the spectrum observed for the native yeast oxidase is very similar to that of the beef heart protein. The two signals seen at 21.7 and 19.7 MHz are due to strongly coupled protons and correspond to proton hyperfine couplings of 16.2 and 12.2 MHz. That these signals are due to the methylene protons of cysteine may be ascertained by noting the intensity change in the ENDOR signals in this region upon deuterium substitution. However, it is not clear whether these two signals arise from methylene protons on the same cysteine ligand or from methylene protons on two different cysteine ligands. Comparison of these signals with those in model sulfur radicals shows [22] that in the latter case the unpaired spin density on the cysteinyl sulfurs ranges from 14 to 37% for one cysteine and from 23 to 52% for the other cysteine. Assuming, however, that the two protons seen by ENDOR are from the same cysteine ligand, only two distinct solutions are possible, placing either 23 or 83% of one unpaired spin on sulfur. Experiments are currently in progress to incorporate cysteine substituted with ^{13}C at the methylene carbon into yeast cytochrome *c* oxidase in order to unambiguously measure the unpaired spin density on the cysteinyl sulfur ligand(s) to Cu_A. As noted previously, the assignment of both strongly coupled protons to a single cysteine ligand would not preclude the existence of a second cysteine ligand to Cu_A. In fact, a substantial delocalization of charge onto copper in oxidized Cu_A would require the presence of a second polarizable ligand such as a second cysteine [20].

The two signals seen at 7.1 and 9.2 MHz in the native enzyme are split by twice the characteristic ^{14}N Zeeman energy ($2\nu_{^{14}N} = 2.00$ MHz) and can be assigned to a ^{14}N with hyperfine coupling of 16 MHz. This assignment was confirmed by the ENDOR spectrum of the (^{15}N)His yeast enzyme. Comparison of the ENDOR spectra for the (^{15}N)His and native yeast proteins reveals that only the intensities of the ^{14}N ENDOR signals at 7 and 9 MHz are substantially reduced by the isotopic substitution of the imidazole ring nitrogens. Due to the difference in nuclear magnetic moment between the two nitrogen isotopes, substitution of the ^{14}N nucleus by ^{15}N would replace the ^{14}N ENDOR signals at 7 and 9 MHz by ^{15}N ENDOR signals at 10 and 13 MHz, respectively. The increased intensity observed in the 10–15 MHz region in the ENDOR spectra of the (^{15}N)His protein is consistent with the appearance of these ^{15}N ENDOR signals. From these observations, it is clear that there is at least one histidine and one cysteine ligand to Cu_A in cytochrome *c* oxidase.

The saturation characteristics of the Cu_A EPR signal are also unusual. The temperature dependence of the relaxation rate of this site is unlike that of any copper-containing proteins or model compounds which we have studied and more closely parallels that of Fe_a or cytochrome *c* [23]. This observation has led us to propose that the EPR relaxation of Cu_A is enhanced by its proximity to one of the iron centers in the enzyme.

We have recently confirmed that the magnetic relaxation of Cu_A is influenced by interaction with another metal site in the enzyme by studying the power saturation of the Cu_A signal in partially reduced enzyme species. In two-electron-reduced, CO-associated cytochrome oxidase, the oxygen reduction site is

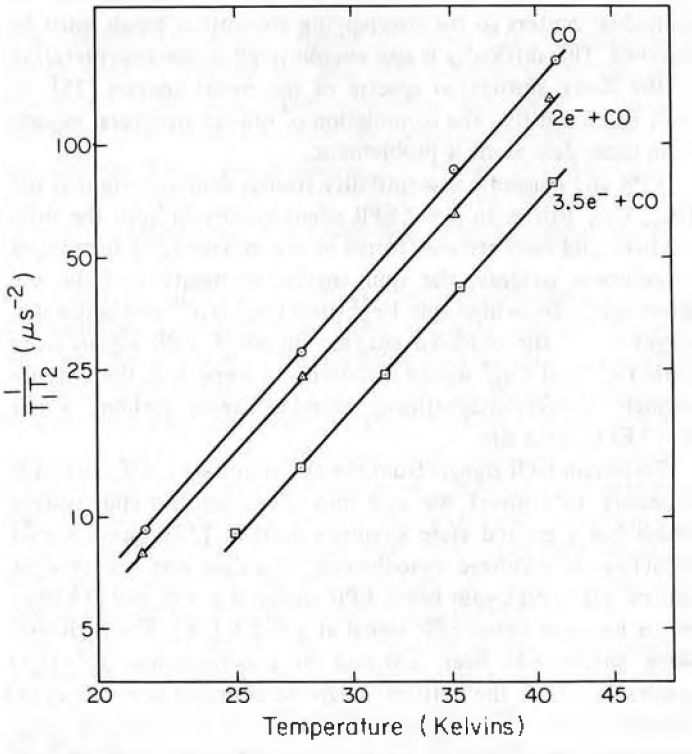

Fig. 4. Saturation behavior at several temperatures of the Cu_A EPR signal in partially reduced CO-associated cytochrome *c* oxidase species. The quantity $1/T_1T_2$ was determined by a least-squares fit to the equation:

$$\text{signal intensity} = \gamma = \gamma_0\left(\frac{P}{1+\alpha P}\right)^{1/2}$$

where α is proportional to T_1T_2. The number of equivalents of reductant added (electrons, e^-) was based on measured heme A concentrations by assuming $4e^-$ per aa_3 unit.

diamagnetic. However, the EPR saturation behavior of Cu_A in this species is only slightly different from that observed in the native enzyme (Fig. 4); we attribute this small difference to a partial (10–15%) reduction of Fe_a which was observed in these samples. When more (*ca.* 1.5 additional) reducing equivalents are added, a much larger effect, corresponding to an approximately two-fold increase in T_1T_2, is observed (Fig. 4). In this sample, both Fe_a and Cu_A are about 75% reduced. Assuming that the redox potentials of Fe_a and Cu_A are uncorrelated, this means that most (*ca.* 75%) of the Cu_A signal remaining in this sample originates from cytochrome oxidase molecules in which Fe_a is reduced and therefore diamagnetic. The change observed in the T_1T_2 of the Cu_A signal may therefore be attributed to the loss of a relaxation pathway involving a magnetic dipolar interaction of this site with Fe_a. Since the effective range of such an interaction is not likely to be greater than about 15 Å, we can estimate that Cu_A and Fe_a are within 15 Å of each other. The absence of a comparable effect when the Cu_B–Fe_{a_3} site is rendered diamagnetic indicates that this site is substantially further removed from Cu_A, particularly since this rapidly relaxing, $S = 2$ site is expected to more efficiently relax other sites than does Fe_a ($S = \frac{1}{2}$).

Cytochrome a_3 and copper B

Although the binding of externally added ligands to the oxygen binding site of cytochrome oxidase has been studied for many years (see, for example, the extensive review by Lemberg [24]), the structure of this site and the details of the reactions that occur there had remained enigmatic. Optical absorption studies of the hemes have proven extremely useful, but care must be exercised in their interpretation because the contribution of individual centers to the overlapping absorption bands must be resolved. This difficulty is also encountered in the interpretation of the X-ray absorption spectra of the metal centers [25], to such an extent that the formulation of unique structural models from these data alone is problematic.

EPR and magnetic susceptibility studies demonstrate that the Fe_{a_3}, Cu_B pair is an $S = 2$ EPR silent species in both the fully oxidized and fully reduced forms of the enzyme [26]. In reduced cytochrome oxidase, the spin angular momentum of the site arises solely from high spin $Fe^{+2}_{a_3}$ since Cu^{+1}_B is d^{10} and hence diamagnetic. In the oxidized enzyme, in which EPR signals from both $Fe^{+3}_{a_3}$ and Cu^{+2}_B would ordinarily be expected, the two are strongly antiferromagnetically coupled, again yielding a net $S = 2$ EPR silent site.

To obtain EPR signals from the cytochrome a_3–Cu_B site, it is necessary to convert the site into a half-integral spin system which has a ground state Kramer's doublet [27]. Upon partial reduction of oxidized cytochrome *c* oxidase one observes, at neutral pH, a high-spin heme EPR signal at $g = 6$, and at higher pH, a low-spin heme EPR signal at $g = 2.6$ [28]. The high-spin heme species has been assigned to a cytochrome $a^{+3}_3 \cdot H_2O$ species in which the antiferromagnetic coupling between cytochrome a_3 and Cu_B has been eliminated by reduction of Cu_B; increasing the pH merely leads to deprotonation of the bound water to form the low-spin cytochrome $a^{+3}_3 \cdot OH^-$ species.

The antiferromagnetic coupling between Cu_B and Fe_{a_3} can also be disrupted by the addition of exogenous ligands. In our laboratory, we have probed the structure of the oxygen binding site by using the paramagnetic ligand nitric oxide (NO) to bind to, and generate EPR signals from, both Fe_{a_3} and Cu_B. The EPR signal observed when NO is added to reduced cytochrome *c* oxidase is typical of that observed for other nitrosylferroheme proteins such as the NO adducts of cytochrome *c*, hemoglobin, or cytochrome *c* peroxidase [29]. In particular, nitrogen superhyperfine splittings are observed for both the NO nitrogen and an endogenous nitrogen bound axially to Fe_{a_3} opposite the NO (Fig. 5). The *g*-values for this complex as well as the magnitudes of the ^{14}N hyperfine splittings indicate that the endogenous nitrogen ligand of Fe_{a_3} is most likely from an imidazole ring. Unambiguous identification of histidine as the endogenous axial ligand to cytochrome a_3 [30] was obtained from the nitrosylferrocytochrome a_3 complex prepared from the (^{15}N)His) yeast oxidase described earlier.

When ^{14}NO is bound to ferrocytochrome a_3 of the yeast enzyme, the $g = 2.006$ component of the EPR signal of the complex exhibits a nine-line hyperfine pattern which can be interpreted in terms of the superposition of three sets of three lines arising from two nonequivalent nitrogens ($I = 1$) interacting with the unpaired electron. The larger of the two hyperfine coupling constants is 20.8 G and the smaller 6.9 G. When ^{15}NO is used in this experiment, the ^{15}NO-bound protein exhibits an EPR spectrum with *g*-values identical to those of the ^{14}NO-bound species, but the $g = 2.006$ component shows a hyperfine pattern consisting of two sets of three lines. This pattern is consistent with the presence of one ^{14}N and one ^{15}N nitrogen bound axially to cytochrome a_3 with a 28.2 G splitting for the ^{15}N and a 7.0 G splitting for the ^{14}N ligand. These spectra of the NO-bound native yeast protein are compared with those of the ^{14}NO- and ^{15}NO-bound (^{15}N)His yeast cytochrome *c* oxidase in Fig. 5. It is apparent from this comparison that the hyperfine patterns have been altered upon (^{15}N)His substitution. The (^{15}N)His ^{15}NO-bound protein hyperfine pattern consists of two sets of doublets, with a ^{15}NO nitrogen splitting of 27.5 G and a splitting of about 12 G for the ^{15}N nitrogen of the histidine. The (^{15}N)His ^{14}NO-bound protein hyperfine pattern consists of three sets of doublets, with splitting of 21 G and 10.2 G for the ^{14}NO and histidine ^{15}N nitrogen, respectively. These studies provide unequivocal identification of histidine as the endogenous fifth ligand to cytochrome a_3.

Although most ferric hemoproteins do not bind NO, fully oxidized cytochrome oxidase exhibits new EPR signals in the presence of NO [31–33]. Signals which are characteristic of high-spin heme (g_x, $g_y \simeq 6$) can be generated by adding NO to oxidized cytochrome oxidase (Fig. 6(b)) or to the fluoride complex of the oxidized enzyme (Fig. 6(c)). A low-spin ($g_z \simeq 3.5$) signal is observed when the cyanide complex of the oxidized enzyme is treated with NO (Fig. 6(d)). These spin states are consistent with what is known about the binding of F^- and CN^- to Fe_{a_3} in the absence of NO [8, 26]. It is therefore apparent that NO binds to Cu_B in the oxidized enzyme, breaking the antiferromagnetic coupling between Cu_B and Fe_{a_3} and thereby permitting the EPR visualization of the Fe_{a_3} center. A Cu^{+2}_B–NO complex most likely possesses a diamagnetic ground state and therefore is not observable by EPR spectroscopy. These observations strongly support the notion that Cu_B as well as Fe_{a_3} can interact with externally added ligands.

The NO complex with the oxidized enzyme can be used to ascertain whether the histidine identified earlier as the axial ligand to Fe_{a_3} in the reduced protein remains coordinated to the heme in the oxidized enzyme. The high-spin heme EPR signal seen at $g \simeq 6$ upon binding of NO to Cu^{+2}_B (Fig. 6(b)) arises from the $M_s = 1/2$ component (Kramer's doublet) of the $S = 5/2$ spin manifold when the applied field is in the plane of the porphyrin

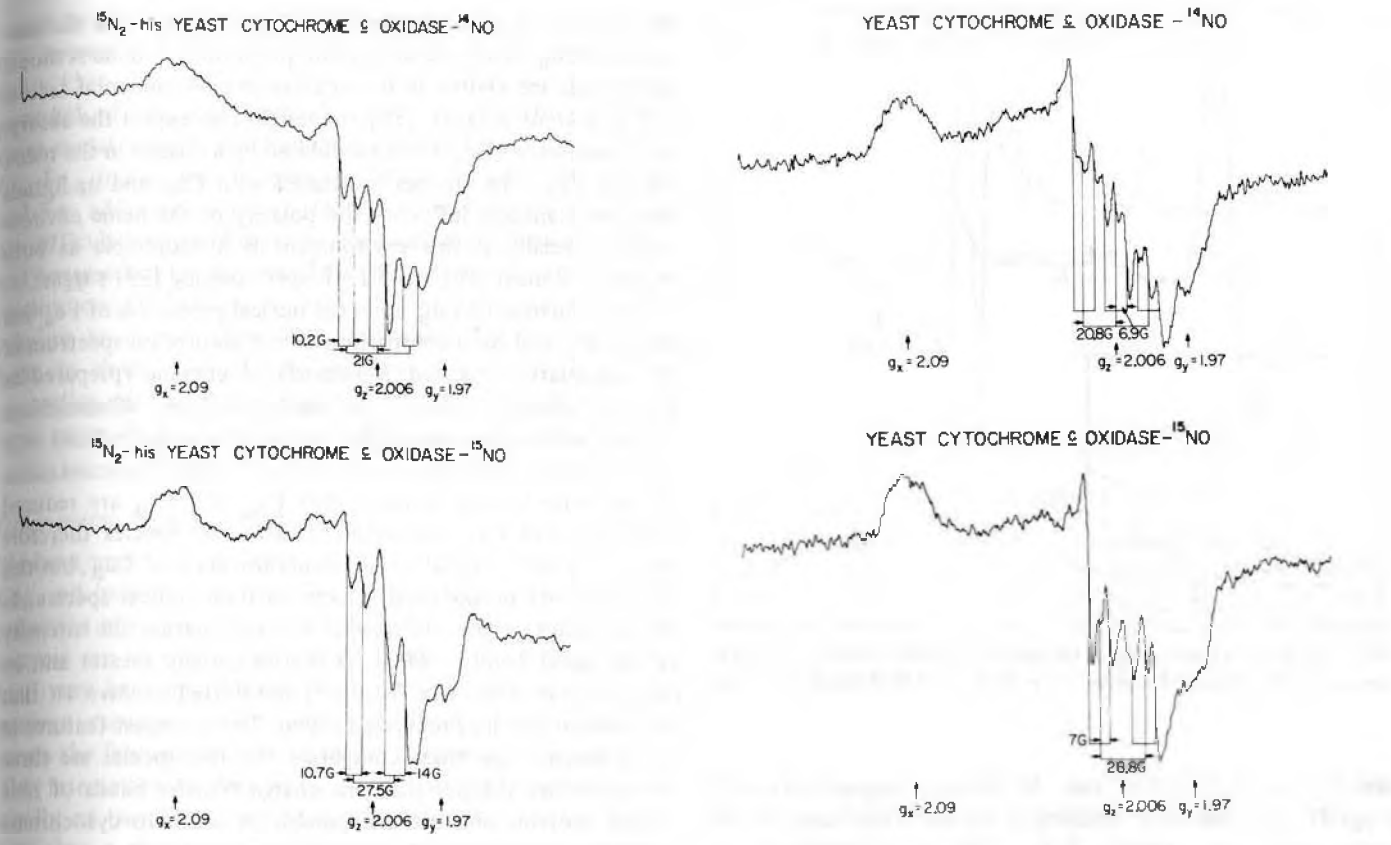

Fig. 5. EPR spectra of the ^{14}NO and ^{15}NO complexes of reduced native and (^{15}N)His yeast cytochrome *c* oxidase. Frequency, 9.2 GHz; temperature, 30 K.

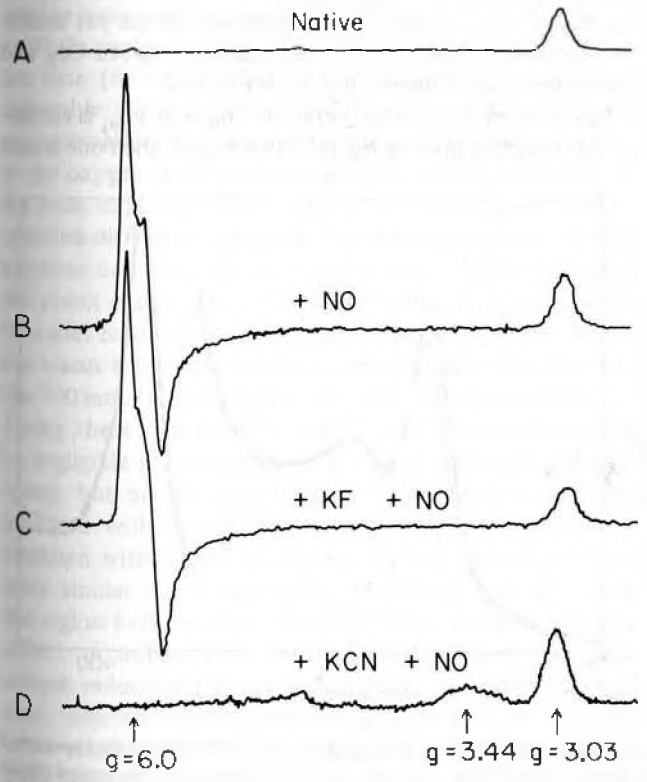

Fig. 6. EPR spectra of beef heart cytochrome *c* oxidase with added ligands. A: no added ligands. B: plus NO (0.9 atm). C: plus KF (1 M) and NO (0.9 atm). D: plus KCN (0.1 M) and NO (0.9 atm). Frequency, 9.2 GHz; temperature, 7–12 K.

ring. The intensity of these signals is temperature dependent and can be used to measure the zero field splitting D for the high-spin heme which can, when compared with those of known hemes, in turn be used to infer the nature of the fifth ligand. In the absence of exogenous ligands, we measure D to be 9 cm^{-1}, and in the presence of F^-, $D \simeq 6\,cm^{-1}$ [33]. These zero-field parameters are indicative of a high-spin heme with an axial histidine.

Neither the EPR signal from nitrosylferrocytochrome a_3 nor the high-spin cytochrome a_3 signal provides any information regarding the position of the histidine *vis-a-vis* Cu_B. A bridging imidazole has been proposed to provide the exchange coupling between the two metal centers [34]. However, a triplet EPR signal observed from the one-quarter-reduced NO-bound enzyme (Fig. 7) provides a measure of the interaction between cytochrome a_3 and Cu_B in the nitrosylferrocytochrome a_3, Cu_B(II) complex and indicates that NO must bind between these two metal ions in this complex; in other words, the histidine imidazole of cytochrome a_3 is distal to Cu_B.

In order to obtain the one-quarter-reduced NO-bound enzyme, we exploited the high reduction potential of cytochrome a_3 to activate the disproportionation of N_3^- in the presence of NO according to the overall reaction

ferricytochrome $a_3 + N_3^- + 2NO \rightarrow$

nitrosylferrocytochrome $a_3 + N_2 + N_2O$

The optical spectrum of the resultant nitrosylferrocytochrome a_3 suggests that the imidazole is still in place. The fact that a triplet EPR signal is observed for this complex indicates that NO binds to the ferrocytochrome a_3 and the unpaired e^- on

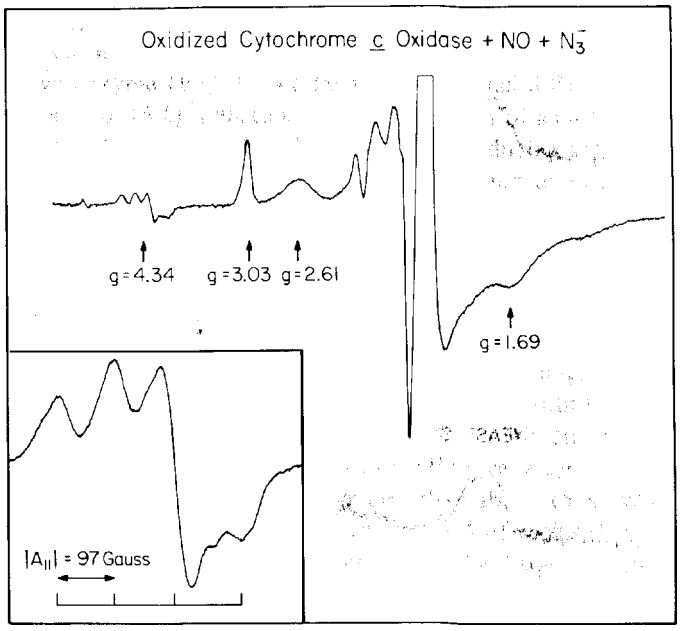

Fig. 7. X-band EPR spectrum of the nitrosylferrocytochrome a_3, Cu_B(II) species at 7 K. (Inset): Magnified view of the half-field transition region.

the NO is sufficiently close to interact magnetically with Cu_B(II). The zero-field splitting D of the triplet can be estimated from the breadth of the $\Delta M_S = \pm 1$ transition. We obtained a value for |D| of 0.07 cm^{-1}. If we assume a purely dipolar interaction between the two spins, we estimate the distance between the two "spin centers" to be 3.4 Å.

The triplet EPR signal from the nitrosylferrocytochrome a_3, Cu_B^{+2} species exhibits copper hyperfine splittings on the half-field transition at $g \sim 4$. The magnitude of the copper hyperfine interaction ($\sim 0.02\,cm^{-1}$) is characteristic of a tetragonal/rhombic geometry for Cu_B. A similar conclusion can be deduced from the results of Reinhammar *et al.* [35], who have subsequently reported a new EPR signal from Cu_B^{+2}. This signal, which is obtained when the enzyme is reoxidized in the presence of bubbling O_2, exhibits a copper hyperfine coupling of 0.011 cm^{-1}. Karlsson and Andreasson [36] have assigned this signal to a $Fe_{a_3}^{+3}$–O_2^- HO^-–Cu_B^{+2} species wherein Cu_B is in an unusual rhombic environment. If this interpretation is correct, then the ligation of O_2 to cytochrome a_3 must raise its reduction potential above that of Cu_B in a manner analogous to that observed in the nitrosylferrocytochrome a_3, Cu_B^{+2} species described above.

The ligands to Cu_B remain uncertain. However, preliminary ENDOR data [37] suggest that there are three nitrogens associated with Cu_B. Comparative ENDOR studies of the native and the ^{15}N(His) yeast oxidase are in progress to ascertain whether these nitrogen ligands to Cu_B originate in histidine imidazoles. Recent EXAFS studies have suggested that there might be a cysteine ligand to Cu_B and that the cysteine sulfur might serve as a bridging ligand between cytochrome a_3 and Cu_B in some states of the oxidized enzyme [25]. Inasmuch as corroborative evidence for this cysteine from EPR and optical measurements is still lacking, the EXAFS result should be considered preliminary.

The data described above indicate that Fe_{a_3} and Cu_B are in close proximity and participate in strong magnetic interactions. While the optical properties of Fe_{a_3} have been the subject of numerous investigations, it has generally been overlooked that these properties might also reflect the proximity of this chromophore to Cu_B. Since the absorption properties of heme A model compounds are known to be sensitive to environmental factors such as solvent polarity [38], one might also expect the absorption spectrum of Fe_{a_3} to be modulated by a change in the redox state of Cu_B. The charges associated with Cu_B and its ligands might substantially influence the polarity of the heme environment, especially if this environment is hydrophobic as both resonance Raman [10] and FT–IR spectroscopy [39] suggest.

The influence of Cu_B upon the optical properties of Fe_{a_3} has been confirmed by a comparison of the absorption spectrum of the one-quarter reduced NO-associated enzyme (prepared as described above) to that of the one-half reduced NO-associated enzyme which is prepared by treating the fully reduced NO-bound protein with ferricyanide (Fig. 8). EPR characterization of the latter species indicates that Fe_{a_3} and Cu_B are reduced while Fe_a and Cu_A are oxidized. The two species therefore differ only with respect to the oxidation state of Cu_B, but this difference has pronounced effects on their optical spectra. In the spectrum of the one-quarter reduced species, the intensity of the alpha band (~ 600 nm) is substantially greater and its position somewhat (*ca.* 70 cm^{-1}) red-shifted relative to that observed in the half-reduced protein. The strongest features in the difference spectrum comparing the two species are three to four times sharper than the charge transfer bands of blue copper proteins and are comparable in width to cytochrome transitions. We therefore assign the observed differences to an influence of the oxidation state of Cu_B upon the absorption properties of Fe_{a_3}. A similar effect has been observed in a chlorophyll model compound when a group on the periphery of the macrocycle is ionized [40]. In this case, the spectral change is almost certainly due to the electrostatic effect of the additional charge upon the wavefunctions of the macrocycle. This suggests that the Cu_B–Fe_{a_3} optical interaction may be simply electrostatic in nature. However, we cannot yet eliminate the possibility that a specific interaction between Cu_B and the NO molecule coordinated to Fe_{a_3} is involved.

If the observed interaction between Cu_B and Fe_{a_3} is electrostatic and does not involve the inhibitor ligand, then one would

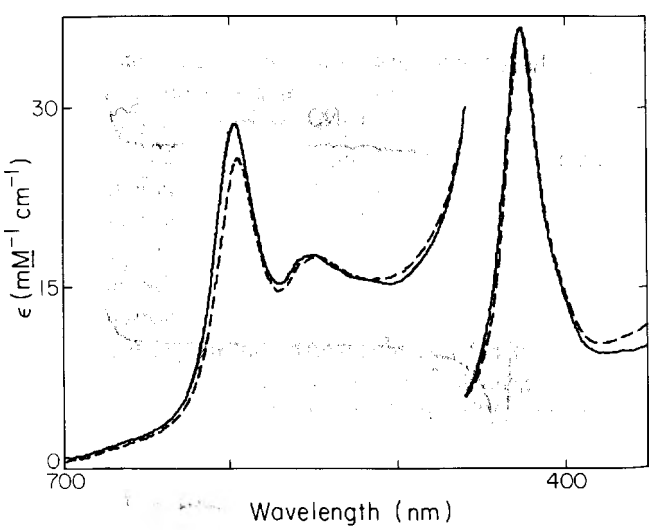

Fig. 8. Absorbance spectra of partially reduced NO-associated species of beef heart cytochrome *c* oxidase in the 700 nm–350 nm region. Solid trace: one-quarter reduced NO-associated species ($Fe_a^{3+}Cu_A^{2+}Cu_B^{2+}Fe_{a_3}^{2+}$·NO). Dashed trace: one-half reduced NO-associated species ($Fe_a^{3+}Cu_A^{2+}Cu_B^{1+}Fe_{a_3}^{2+}$·NO). The vertical scale in the 350–475 nm region is 5x that indicated.

expect it to be manifested in the native protein as well as in the NO derivative. If this is the case, it raises the interesting possibility that the oxidation state of Cu_B influences the redox potential of Fe_{a_3}. A reduction potential interaction between these metal centers has been less frequently proposed than a Fe_a–Fe_{a_3} interaction, in spite of the known proximity of Cu_B and Fe_{a_3}. Measurements of the reduction potential(s) of Cu_B are difficult because this center has no strong optical absorption and because low-temperature EPR data, which can provide information on the oxidation state of Cu_B, are not necessarily relevant to room temperature thermodynamic properties. We hope to characterize the influence of Cu_B upon the optical properties of the native enzyme and exploit this effect to learn more about the redox properties of the Cu_B–Fe_{a_3} couple.

Other metal–metal interactions

We have presented evidence for interactions between Fe_{a_3} and Cu_B and between Fe_a and Cu_A. Interactions between the O_2 reduction site (Fe_{a_3}–Cu_B) and the other metal centers in the enzyme are also of considerable interest since coupling of this kind may have implications for the mechanisms by which the enzyme regulates intramolecular electron transfer and conserves the free energy released in the oxygen reduction reaction. The interaction models which have been proposed are principally of two kinds, involving either interactive redox potentials (i.e., a mechanism in which an oxidation state change in one metal center modifies the reduction potential of other centers) [41, 42] or interactive optical properties (i.e., a mechanism in which an oxidation state change in one metal center modifies the optical absorption spectrum of other metal centers) [43]. In both cases, attention has in the past been focused on interaction between Fe_a and the metals of the oxygen reduction site rather than upon interactions between Cu_A and the oxygen reduction site.

While some available Soret region magnetic circular dichroism data [8] are relevant to the question of spectroscopically detectable interactions between Fe_a and the Cu_B–Fe_{a_3} couple, no systematic study has been made of the influence of changes at the oxygen reduction site upon the optical properties of Fe_a. We have explored this question by recording reduced-minus-oxidized difference spectra of Fe_a in a large number of different inhibitor derivatives of the enzyme which differ with respect to the redox and/or spin state of the metals at the oxygen reduction site. Some of these results are displayed in Fig. 9. Both of the traces shown are reduced-minus-oxidized spectra of Fe_a in the 700 nm–350 nm region (Cu_A also undergoes redox changes during these experiments, but its contribution is expected to be negligible relative to those of Fe_a in this region of the spectrum), but in one case the Cu_B–Fe_{a_3} couple is oxidized and inhibited with cyanide, while in the other it is reduced and inhibited with carbon monoxide. The two spectra are substantially similar but exhibit small differences near 425 nm and in the region between 450 nm and 500 nm. These differences may reflect an influence of the redox and/or ligation state of the oxygen reduction site upon the optical properties of Fe_a; however, they are relatively small in magnitude, and we feel that other effects might be responsible, for example, the presence of small quantities of absorbing impurities or the formation of a small concentration of so-called "pulsed" oxidase during the slow turnover of the cyanide-inhibited enzyme. Thus, while we cannot eliminate the possibility of subtle interactions between

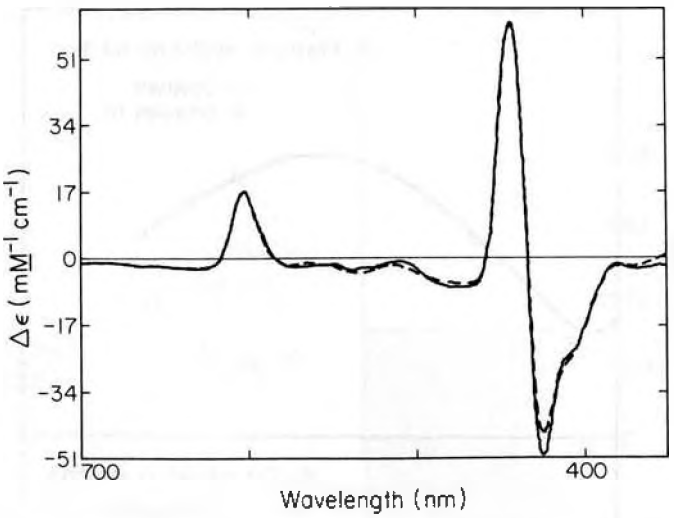

Fig. 9. Reduced-minus-oxidized Fe_A difference spectra obtained by two methods. Dashed trace: the Fe_a difference spectrum obtained using cyanide to stabilize $Fe^{+3}_{a_3}$ and $Cu^{2+}_B(Fe^{2+}_a Cu^{1+}_A Cu^{2+}_B Fe^{3+}_{a_3} \cdot CN^-$ *minus* $Fe^{3+}_a Cu^{2+}_A Cu^{2+}_B Fe^{2+}_{a_3} \cdot CN^-)$. Solid trace: the Fe_a difference spectrum obtained using carbon monoxide to stabilize $Fe^{2+}_{a_3}$ and $Cu^{1+}_B(Fe^{2+}_a Cu^{1+}_A Cu^{1+}_B Fe^{2+}_{a_3} \cdot CO$ *minus* $Fe^{3+}_a Cu^{2+}_A Cu^{1+}_B Fe^{2+}_{a_3} \cdot CO)$.

Fe_a and the oxygen reduction site, it is clear that no strong interaction of this kind is manifested in the optical spectrum.

The absorption spectrum of oxidized cytochrome oxidase has a relatively broad band centered near 825 nm ($\epsilon \simeq 2000\ M^{-1}\,cm^{-1}$) which is eliminated upon reduction of the enzyme. Copper depletion studies [44] indicate that this band is due to one or both of the copper centers. In partially reduced samples of the enzyme monitored by both absorption and EPR spectroscopy, the intensity of this band correlates with the intensity of the Cu_A EPR signal [45], suggesting that this band originates in a charge transfer transition involving Cu_A. However, reflectance spectra of partially reduced inhibitor complexes of the enzyme have been used to support assignment of this band to both Cu_A and Cu_B in roughly equal amounts [46]. In order to investigate this question and to explore the possibility of spectroscopically detectable interactions between Cu_A and the oxygen reduction site, we have employed an approach similar to that described above in connection with Fe_a. Inhibitors were used to stabilize the Cu_B–Fe_{a_3} couple in either the reduced or the oxidized state while the redox states of Cu_A and Fe_a were changed; the effects of these redox changes were studied by calculating oxidized-minus-reduced difference spectra for the 825 nm absorbance. Some of our results are given in Fig. 10 together with Gaussian fits to the spectra. A primary implication of these experimental results is that the 825 nm band does not contain a substantial contribution due to Cu_B or Fe_{a_3}. The change in extinction accompanying reduction of Cu_A and Fe_a is very close to $2000\ M^{-1}\,cm^{-1}$ and thus is comparable to the change accompanying the transition of the enzyme from the fully oxidized to the fully reduced state. This conclusion is more directly substantiated by our observation (data not shown) that the near-infrared spectrum of the half-reduced carbon monoxide complex of the enzyme is superimposable upon that of the fully oxidized enzyme. These results are in contrast to those reported in the reflectance spectroscopy study of Powers *et al.* [46]. Another important conclusion is that the oxidized-minus-reduced absorbance at 825 nm is very well fitted by a single Gaussian, which is consistent with assignment to an

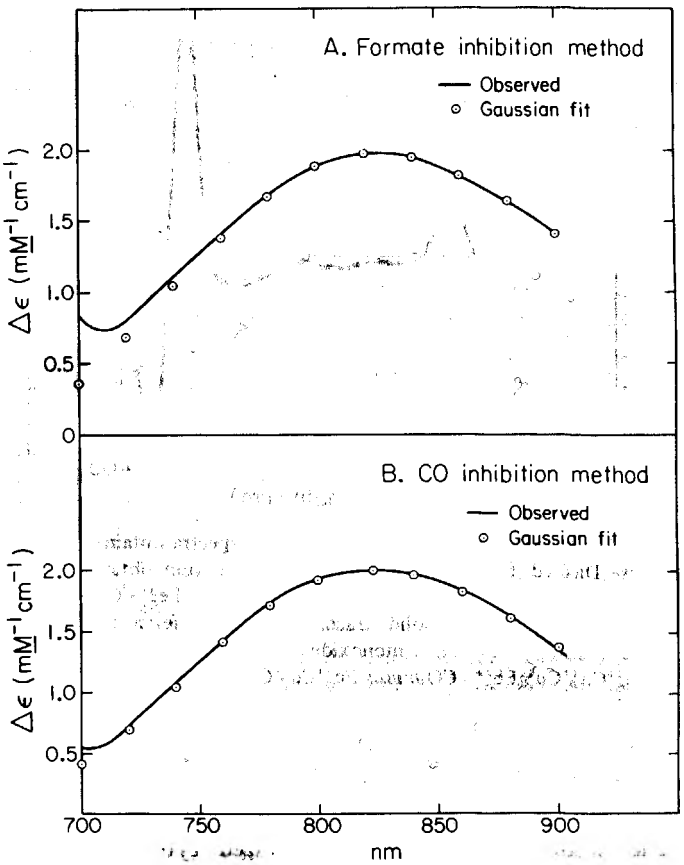

Fig. 10. Oxidized-minus-reduced difference spectra of Cu_A obtained by two methods. Top: oxidized-minus-reduced difference spectrum of Cu_A obtained using formate inhibition of Cu_B and Fe_{a_3} ($Fe_a^{+3}Cu_A^{+2}Cu_B^{+2}Fe_{a_3}^{+3} \cdot HCOO^-$ *minus* $Fe_a^{+2}Cu_A^{+1}Cu_B^{+2}Fe_{a_3}^{+3} \cdot HCOO^-$). The circles represent a Gaussian with $\lambda_{max} = 825$, hwhh $= 1.43 \times 10^3\,cm^{-1}$. Bottom: oxidized-minus-reduced difference spectrum of Cu_A obtained using CO inhibition of Cu_B and Fe_{a_3}($Fe_a^{+3}Cu_A^{+2}Cu_B^{+1}Fe_{a_3}^{+2} \cdot CO$ *minus* $Fe_a^{+2}Cu_A^{+1}Cu_B^{+1}Fe_{a_3}^{+2} \cdot CO$). The circles represent a Gaussian with $\lambda_{max} = 823$, hwhh $= 1.41 \times 10^3\,cm^{-1}$.

individual charge transfer band from one metal center. Finally, it is apparent that changes in the redox and ligation state of the Cu_B–Fe_{a_3} couple do not significantly influence the energy, the intensity, or the width of this transition. These parameters are expected to be quite sensitive to the details of the Cu_A site geometry, so this result indicates that the structure of this site is not substantially affected by changes in redox state, spin state, or ligation of the oxygen reduction site.

The available visible and near-infrared absorption data thus suggest that there is little, if any, evidence for structural coupling between the Cu_B–Fe_{a_3} site and the other metal centers. Important structural interactions which are not detectable by this method may nevertheless occur, particularly in the case of Fe_a, since the optical properties of the heme may be relatively insensitive to many environmental factors. Furthermore, there is some evidence, for example, from MCD studies [42], that the reduction potential of Fe_a is strongly influenced by the redox state of Fe_{a_3}; presumably this involves some change in the structure of either ferrous or ferric Fe_a. We feel that this important problem requires further study and accordingly plan to explore this matter in greater detail in the future.

Structural model

We present in Fig. 11 a model for oxidized cytochrome *c* oxidase. This model summarizes the structural results obtained to date.

Generally speaking, the metal centers can be grouped into two pairs: (1) Fe_a and Cu_A, and (2) the O_2 reduction site, composed of Fe_{a_3} and Cu_B. The EPR relaxation studies described above show that cytochrome *a* and Cu_A are within ~ 15 Å of each other. The close proximity of Fe_{a_3} and Cu_B in the O_2 reduction site is now well established. The distance between them seems to be about 5 Å, but quite likely varies with the state of the enzyme. It seems clear that this proximity is critical for efficient electron transfer and for the stabilization of O_2 reduction intermediates during the O_2 reduction process. On the other hand, the two pairs of metal ions seem to be relatively far apart, as we have been unable to detect by EPR any substantial effect of the spin state of the O_2 reduction site on the EPR relaxation behavior of cytochrome *a* or Cu_A.

There now exists convincing evidence that Fe_a and Cu_A are located near the cytosol side of the mitochondrial membrane [2, 6], where cytochrome *c* is known to bind. The location of the O_2 reduction site is, however, less certain. Recently, we obtained preliminary EPR results which place Fe_{a_3} and Cu_B closer to the matrix side than the cytosol side of the mitochondrial membrane. This location of the oxygen reduction site is reasonable, since the consumption of matrix-derived protons in the reduction of oxygen will contribute to the electrochemical gradient across the inner mitochondrial membrane.

In terms of function, the general consensus is that Fe_a and Cu_A serve to accept electrons from cytochrome *c* and transfer them to the O_2 reduction site. However, the exact sequence of this electron transfer remains unsettled, in part due to the rapid redox equilibrium which exists bween these two centers [47]. The rate determining step in the overall O_2 reduction process is probably electron transfer between the Fe_a/Cu_A pair and the O_2 reduction site [48]. It has been known for some time that the turnover rate is sensitive to environmental factors, including the fluidity of the lipid medium in which the protein is embedded [49]. In view of this sensitivity and the apparently large distance over which the electrons must transfer between Fe_a/Cu_A and the O_2 reduction site, we surmise that this electron transfer process may be coupled to some conformational change which serves not only to control directed electron transfer over the relatively large distance between the two metal ion pairs, but to couple the redox energy to the pumping of protons across the mitochondrial membrane.

Mechanism of oxygen reduction

Our structural results on Fe_{a_3} and Cu_B lend considerable insight into the role that these two metal centers play in the O_2 reduction process. The observation that the binding of O_2 raises the reduction potential of Fe_{a_3} above that of Cu_B has suggested to us that the role of Fe_{a_3} might be to anchor O_2 and its reduction intermediates, at least during the early stages of O_2 reduction. Cu_B would then serve to transfer electrons into the site. The close proximity of the two metal ions may serve both to facilitate electron transfer and to stabilize reactive intermediates. On the basis of these considerations we proposed some years ago [32] a mechanism for dioxygen reduction which involves both a peroxo and a ferryl intermediate. Since that time, new evidence has been obtained in support of this mechanism, and additional results pertinent to the rest of the cycle have become available.

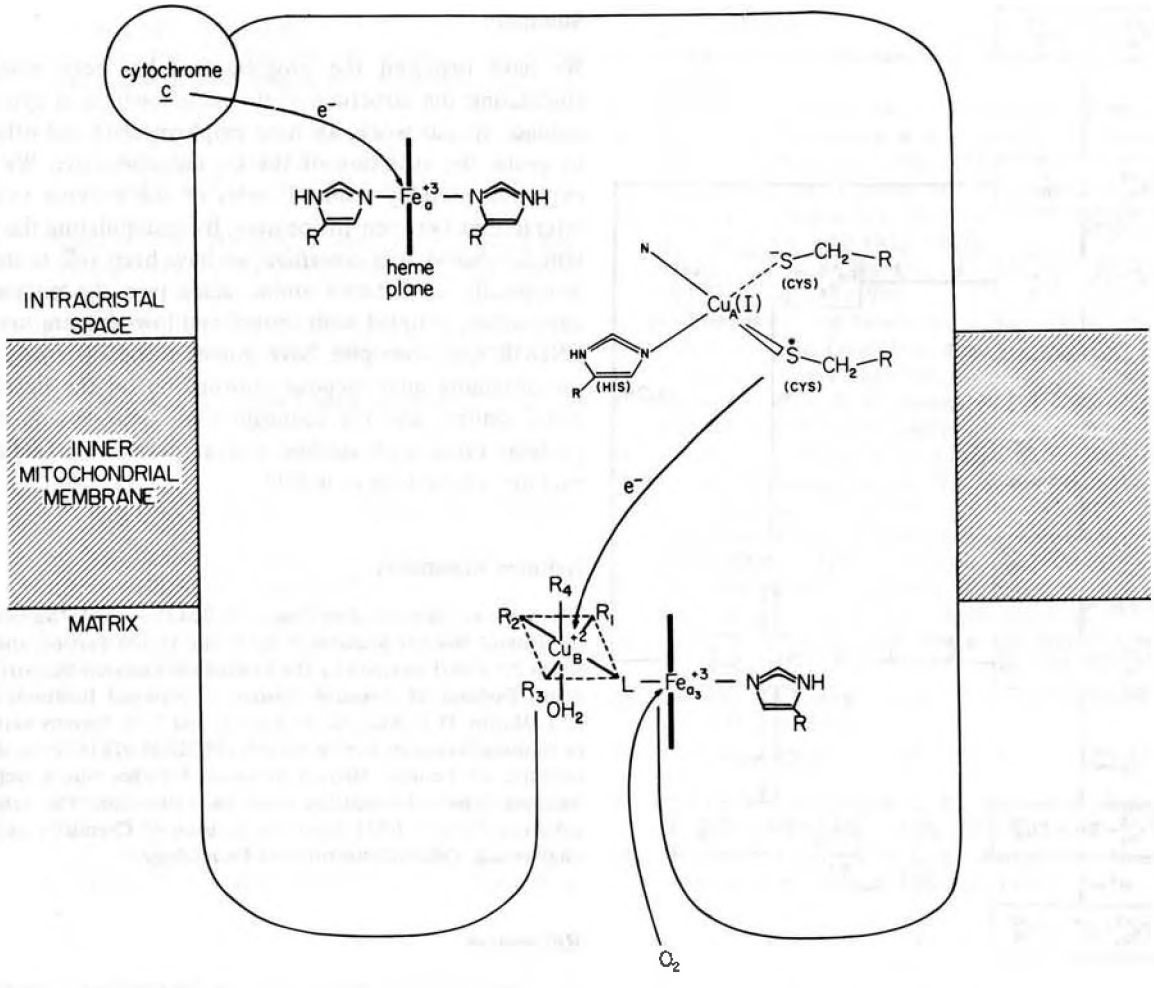

Fig. 11. A model for oxidized cytochrome *c* oxidase.

An elaborated version of our earlier proposed scheme is presented in Fig. 12. For clarity, only the Fe_{a_3}–Cu_B site is shown.

The scheme begins with the binding of O_2 to reduced Fe_{a_3}. This is followed by the rapid transfer of an electron from Cu_B to yield an intermediate which is, at least formally, equivalent to peroxide bound to the oxidized site. The proposal of such an intermediate has recently gained support from the observation [50] that oxidized cytochrome *c* oxidase binds hydrogen peroxide tightly ($K_d \sim 10\,\mu M$). It is likely that the bonding in this first intermediate resembles that in the oxidized enzyme–peroxide complex. In recent optical experiments in our laboratory, we have noted a close spectroscopic similarity between the peroxide adduct of the oxidized enzyme and the species formed by the addition of oxygen to the two-electron reduced enzyme. These species merit further study by resonance Raman and other spectroscopic methods.

The next step in the sequence is the transfer of an electron from Fe_a/Cu_A to the O_2 reduction site. In our earlier formulation, we proposed that the transfer of this electron leads to rupture of the oxygen–oxygen bond and the formation of a ferryl species adjacent to Cu_B^{+2}. Indeed, evidence for such an intermediate has since been reported by Karlsson *et al.* [51]. In studies of the low-temperature reoxidation of the reduced enzyme, they reported the observation of an EPR signal from Cu_B^{+2} with unusual relaxation properties. In this intermediate, Cu_B^{+2} appears to be influenced by a nearby rapidly relaxing paramagnetic center such as Fe(IV), consistent with our previously proposed intermediate.

To complete the reduction of dioxygen, a second electron is transferred to the site from Fe_a/Cu_A. This results in the formation of a species in which both metal ions of the O_2 reduction site are in the oxidized state. In limited turnover experiments, Brudvig *et al.* [33] have shown that this species can relax slowly in succession to a number of "dead end" forms of the oxidized enzyme. In the scheme presented here, the first such species is denoted as "oxygenated." It is characterized by rather strong antiferromagnetic exchange coupling between Fe_{a_3} and Cu_B which is mediated by a readily exchangeable bridging ligand, possibily the hydroxide anion. According to Brudvig *et al.* [33], this form of the enzyme decays slowly ($t_{1/2} \sim 1$ h) to another form which exhibits an X-band EPR signal near $g \sim 12$. The bridging ligand in this "g12" species was found to be almost substitutionally inert, and it has been proposed that the strongly bound bridging ligand is a μ-oxo.

The reduction of O_2 is a very rapid and efficient process. Accordingly, the direct observation of O_2 reduction intermediates is difficult. Chance *et al.* [52] have developed a low-temperature trapping technique capable of stabilizing several of the intermediate species, allowing them to be probed spectroscopically. With this technique, Clore *et al.* [53, 54] recently completed a careful study of the intermediates involved in O_2 reduction and characterized them using optical and EPR spectroscopies. Starting from either the fully reduced enzyme or the mixed valence state in which only Fe_{a_3} and Cu_B are reduced, they have characterized three species which appear to correspond well spectroscopically and kinetically with the first three

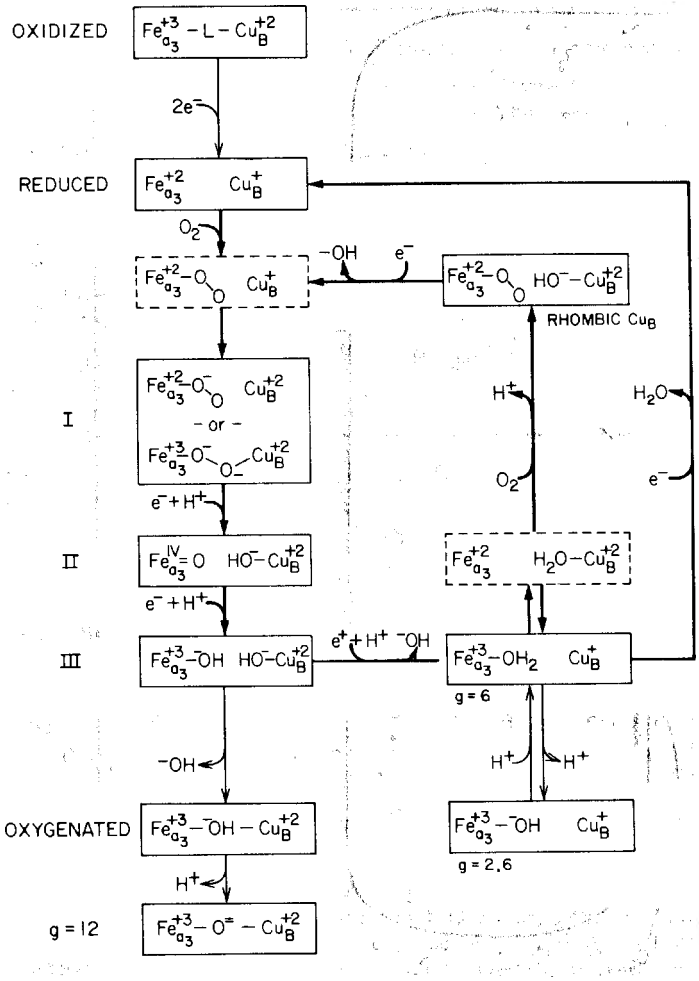

Fig. 12. Proposed mechanism for the reduction of dioxygen by cytochrome *c* oxidase. For clarity, only the metal centers of the oxygen binding site are shown.

intermediates described in our mechanistic scheme. Accordingly, we have adopted the nomenclature of Clore *et al.* to describe these intermediates. Intermediate I of their study would correspond to our "peroxo-like" species; intermediate II to our ferryl species; and intermediate III to a form of the oxidized site immediately following the final electron transfer.

In the cycling enzyme, we expect Fe_a and/or Cu_A to be reduced. If this is so, the O_2 reduction site may then accept another electron from Fe_a/Cu_A to form a partially reduced form of the site. We expect the resultant species to give the high-spin heme EPR signal at $g \sim 6$ and, at higher pH, a low-spin heme EPR signal at $g \sim 2.6$. The fate of this intermediate depends on the relative availability of O_2 and reducing equivalents. Under low oxygen tension, the site can accept an electron from Fe_a/Cu_A to re-form the fully reduced site and complete the cycle. In the presence of excess O_2, however, binding of O_2 can stabilize the $Fe_{a_3}^{+2}$–O_2, Cu_B^{+2} species faster than electron transfer from Fe_a/Cu_A. The EPR spectrum of this site would then be expected to show only a normal Cu_B^{+2} EPR signal. It is precisely this species which we assign to the rhombic Cu_B^{+2} EPR signal observed by Reinhammar *et al.* [35] upon reoxidation of the reduced enzyme in the presence of bubbling O_2. Subsequent electron transfer from Fe_a/Cu_A would lead quickly to intermediate I and a continuation of the O_2 reduction cycle.

Summary

We have reviewed the progress that has been made toward elucidating the structure of the metal centers in cytochrome *c* oxidase. In our work, we have employed NO and other ligands to probe the structure of the O_2 reduction site. We have also exploited partially reduced states of the enzyme to study the interactions between the centers. By manipulating the yeast system *Saccharomyces cerevisiae*, we have been able to incorporate isotopically substituted amino acids into the enzyme. These approaches, coupled with optical and low-temperature EPR and ENDOR spectroscopies, have proven to be extremely powerful for obtaining unambiguous information on the ligands of the metal centers and the disposition of these centers within the protein. From such studies, a clear picture of the functioning enzyme is beginning to unfold.

Acknowledgements

This work was supported by Grant GM-22432 from the National Institute of General Medical Sciences, U.S. Public Health Service, and by BRSG Grant RR07003 awarded by the Biomedical Research Support Grant Program, Division of Research Resources, National Institutes of Health. C. T. Martin, D. F. Blair, G. W. Brudvig and T. H. Stevens were recipients of National Research Service Awards (5T32GM-07616) from the National Institute of General Medical Sciences. J. Gelles was a recipient of a National Science Foundation Graduate Fellowship. This article is Contribution Number 6721 from the Division of Chemistry and Chemical Engineering, California Institute of Technology.

References

1. Lehninger, A. L., *Biochemistry*. Worth Publishers, New York (1975).
2. Wikström, M., Krab, K. and Saraste, M., *Cytochrome Oxidase*. Academic Press, London (1981).
3. Wikström, M. and Krab, K., *Biochim. Biophys. Acta* **549**, 177 (1979).
4. Azzi, A., *Biochim. Biophys. Acta* **594**, 231 (1980).
5. Henderson, R., Capaldi, R. A. and Leigh, J. S., *J. Mol. Biol.* **112**, 631 (1977).
6. Blum, H., Leigh, J. S. and Ohnishi, T., *Biochim. Biophys. Acta* **626**, 31 (1980).
7. Andréasson, L. -E., *Eur. J. Biochem.* **53**, 591 (1975).
8. Babcock, G. T., Vickery, L. E. and Palmer, G., *J. Biol. Chem.* **251**, 7907 (1976).
9. van Gelder, B. F. and Beinert, H., *Biochim. Biophys. Acta* **189**, 1 (1969).
10. Babcock, G. T., Callahan, P. M., Ondrias, M. R. and Salmeen, I., *Biochemistry* **20**, 959 (1981).
11. Peisach, J., in *Frontiers of Biological Energetics* (Edited by P. L. Dutton, J. S. Leigh, Jr and A. Scarpa), Vol. 2, pp. 873–881. Academic Press, New York (1978).
12. Chan, S. I., Bocian, D. F., Brudvig, G. W., Morse, R. H. and Stevens, T. H., in *Cytochrome Oxidase* (Edited by T. E. King, Y. Orii, B. Chance and K. Okunuki), pp. 177–188. Elsevier, Amsterdam (1979).
13. Aasa, E., Albracht, S. P. J., Falk, K. -E., Lanne, B. and Vänngård, T., *Biochim. Biophys. Acta* **422**, 260 (1976).
14. Greenaway, F. T., Chan, S. H. P. and Vincow, G., *Biochim. Biophys. Acta* **490**, 62 (1977).
15. Abragam, A. and Bleaney, B., *Electron Paramagnetic Resonance of Transition Ions*. Oxford Press, London (1970).
16. Hu, V. W., Chan, S. I. and Brown, G. S., *Proc. Natl. Acad. Sci. U.S.A.* 74, 3821 (1977).
17. Chan, S. I., Bocian, D. F., Brudvig, G. W., Morse, R. H. and Stevens, T. H., in *Frontiers of Biological Energetics* (Edited by P. L. Dutton, J. S. Leigh, Jr. and A. Scarpa), Vol. 2, pp. 883–888. Academic Press, New York (1978).
18. Hoffman, B. M., Roberts, J. E., Swanson, M., Speck, S. H. and Margoliash, E., *Proc. Natl. Acad. Sci. U.S.A.* 77, 1452 (1980).
19. Van Camp, H. L., Wei, Y. H., Scholes, C. P. and King, T. E., *Bio-*

chim. Biophys. Acta 537, 238 (1978).
20. Hemmerich, P., in *The Biochemistry of Copper* (Edited by J. Peisach, P. Aisen and W. E. Blumberg), pp. 15–34. Academic Press, New York (1966).
21. Stevens, T. H., Martin, C. T., Wang, H., Brudvig, G. W., Scholes, C. P. and Chan, S. I., *J. Biol. Chem.* 257, 12106 (1982).
22. Hadley, J. H., Jr. and Gordy, W., *Proc. Natl. Acad. Sci. U.S.A.* 74, 216 (1977).
23. Chan, S. I., Brudvig, G. W., Martin, C. T. and Stevens, T. H., in *Electron Transport and Oxygen Utilization* (Edited by C. Ho), Elsevier, Amsterdam (in press) (1982).
24. Lemberg, M. R., *Physiol. Rev.* 49, 48 (1969).
25. Powers, L., Chance, B., Ching, Y. and Angiolillo, P., *Biophys. J.* 34, 465 (1981).
26. Tweedle, M. F., Wilson, L. J., García-Iñiguez, L., Babcock, G. T. and Palmer, G., *J. Biol. Chem.* 253, 8065 (1978).
27. Wertz, J. E. and Bolton, J. R., *Electron Spin Resonance*. McGraw-Hill, New York (1972).
28. Hartzell, C. R. and Beinert, H., *Biochim. Biophys. Acta* 368, 318 (1974).
29. Yonetani, T., Yamamoto, H., Erman, J. E., Leigh, J. S., Jr. and Reed, G. H., *J. Biol. Chem.* 247, 2447 (1972).
30. Stevens, T. H. and Chan, S. I., *J. Biol. Chem.* 256, (1981).
31. Stevens, T. H., Brudvig, G. W., Bocian, D. F. and Chan, S. I., *Proc. Natl. Acad. Sci. U.S.A.* 76, 3320 (1979).
32. Brudvig, G. W., Stevens, T. H. and Chan, S. I., *Biochemistry* 19, 5275 (1980).
33. Brudvig, G. W., Stevens, T. H., Morse, R. H. and Chan, S. I., *Biochemistry* 20, 3912 (1981).
34. Palmer, G., Babcock, G. T. and Vickery, L. E., *Proc. Natl. Acad. Sci. U.S.A.* 73, 2206 (1973).
35. Reinhammar, B., Malkin, R., Jensen, P., Karlsson, B., Andréasson, L. -E., Aasa, R., Vänngård, T. and Malmström, B. G., *J. Biol. Chem.* 255, 5000 (1980).
36. Karlsson, B. and Andréasson, L. -E., *Biochim. Biophys. Acta* 635, 73 (1981).
37. Hoffman, B. and Reinhammar, B., Private communication.
38. Babcock, G. T., Ondrias, M. R., Gobeli, D. A., Van steelandt, J. and Leroi, G. E., *FEBS Lett.* 108, 147 (1979).
39. Yoshikawa, S. and Caughey, W. S., *J. Biol. Chem.* 247, 412 (1982).
40. Davis, R. C., Ditson, S. L., Fentiman, A. F. and Pearlstein, R. M., *J. Am. Chem. Soc.* 103, 6823 (1981).
41. Wikstrom, M. K. F., Harmon, H. J., Ingledew, W. J. and Chance, B., *FEBS Lett.* 65, 259 (1976).
42. Carithers, R. P. and Palmer, G., *J. Biol. Chem.* 256, 7967 (1981).
43. Wilson, D. F. and Leigh, J. S., *Ann. N.Y. Acad. Sci.* 227, 630 (1974).
44. Wharton, D. C. and Tzagoloff, A., *J. Biol. Chem.* 239, 2036 (1964).
45. Beinert, H., Shaw, R. W., Hansen, R. E. and Hartzell, C. R., *Biochim. Biophys. Acta* 591, 458 (1980).
46. Powers, L., Blumberg, W. E., Chance, B., Barlow, C. H., Leigh, J. S., Jr., Smith, J., Yonetani, T., Vik, S. and Peisach, J., *Biochim. Biophys. Acta* 546, 520 (1979).
47. Andréasson, L. -E., Malmström, B. G., Strömberg, C. and Vänngård, T., *FEBS Lett.* 28, 297 (1972).
48. Gibson, Q. H. and Greenwood, C., *J. Biol. Chem.* 240, 2694 (1965).
49. Vik, S. B. and Capaldi, R. A., *Biochemistry* 16, 5755 (1977).
50. Bickar, D., Bonaventura, J. and Bonaventura, C., *Biochemistry* 21, 2661 (1982).
51. Karlsson, B., Aasa, R., Vänngård, T. and Malmström, B. G., *FEBS Lett.* 131, 186 (1981).
52. Chance, B., Saronio, C. and Leigh, J. S., *J. Biol. Chem.* 250, 9226 (1975).
53. Clore, G. M., Andréasson, L. -E., Karlsson, B., Aasa, R. and Malmström, B. G., *Biochem. J.* 185, 139 (1980).
54. Clore, G. M., Andréasson, L. -E., Karlsson, B., Aasa, R. and Malmström, B. G., *Biochem. J.* 185, 155 (1980).